Title

Proteomic analysis reveals distinctive protein profiles involved in CD8+ T cell-mediated murine autoimmune cholangitis

Journal

Cellular & Molecular Immunology, 15(8)

ISSN

1672-7681

Authors

Zhang, Weici
Zhang, Ren
Zhang, Jun
et al.

Publication Date

2018-08-01

DOI

10.1038/cmi.2017.149

Peer reviewed

Cellular and Molecular Immunology (2018) 15, 756–767

www.nature.com/cmi

RESEARCH ARTICLE

Proteomic analysis reveals distinctive protein profiles involved in CD8+ T cell-mediated murine autoimmune cholangitis

Weici Zhang[1,6], Ren Zhang[1,2,6], Jun Zhang[1,7], Ying Sun[1,3], Patrick SC Leung[1], Guo-Xiang Yang[1], Zongwen Shuai[1,4], William M Ridgway[5] and M Eric Gershwin[1]

Autoimmune cholangitis arises from abnormal innate and adaptive immune responses in the liver, and T cells are critical drivers in this process. However, little is known about the regulation of their functional behavior during disease development. We previously reported that mice with T cell-restricted expression of a dominant negative form of transforming growth factor beta receptor type II (dnTGFβRII) spontaneously develop an autoimmune cholangitis that resembles human primary biliary cholangitis (PBC). Adoptive transfer of $CD8^+$ but not $CD4^+$ T cells into $Rag1^{-/-}$ mice reproduced the disease, demonstrating a critical role for $CD8^+$ T cells in PBC pathogenesis. Herein, we used SOMAscan technology to perform proteomic analysis of serum samples from dnTGFβRII and B6 control mice at different ages. In addition, we analyzed CD8 protein profiles after adoptive transfer of splenic $CD8^+$ cells into $Rag1^{-/-}$ recipients. The use of the unique SOMAscan aptamer technology revealed critical and distinct profiles of CD8 cells, which are key to biliary mediation. In total, 254 proteins were significantly increased while 216 proteins were significantly decreased in recipient hepatic $CD8^+$ cells compared to donor splenic $CD8^+$ cells. In contrast to donor splenic $CD8^+$ cells, recipient hepatic $CD8^+$ cells expressed distinct profiles for proteins involved in chemokine signaling, focal adhesion, T cell receptor and natural killer cell-mediated cytotoxicity pathways.
Cellular and Molecular Immunology advance online publication, 29 January 2018; doi:10.1038/cmi.2017.149

Keywords: autoimmune cholangitis; CD8; dnTGFβRII mice; proteomic analysis

INTRODUCTION

Primary biliary cholangitis (PBC) is a chronic autoimmune liver disease characterized by the destruction of hepatic bile ducts, cholestasis, and anti-mitochondrial Abs (AMAs), leading to fibrosis, cirrhosis, and ultimately, liver failure.[1] Accumulating evidence implicates $CD8^+$ cells in the pathogenesis of PBC.[2,3] $CD8^+$ T cells are directed to the mitochondrial protein PDC-E2 [4] and are significantly enriched in PBC livers.[5,6] Histologically, $CD8^+CD57^+$ T cells responding specifically to the major histocompatibility class I epitope of PDC-E2 accumulate in the periportal area in PBC.[7] A previous genome-wide association study (GWAS) revealed that the cytotoxic T lymphocyte-associated antigen-4 (CTLA-4) gene is significantly associated with PBC;[8] treatment with CTLA-4 antibody reduced hepatic T-cell infiltrates and inhibited biliary cell damage in a mouse model.[9] $CD8^+$ T cells also mediate biliary cell damage and cholangitis in IL-$2R^{-/-}$ mice with defective T regulatory cells.[10,11] We have previously reported that dnTGFβRII mice,[12] spontaneously develop wide-ranging $CD4^+$ and $CD8^+$ lymphocytic liver infiltration, periportal inflammation, production of specific AMAs, and biliary destruction, which are highly similar to the histological features of human PBC.[13] Importantly, adoptive transfer of splenic $CD8^+$ T cells from dnTGFβRII mice into recombinase-deficient ($Rag1^{-/-}$) mice induces increased IFN-γ and TNF-α production, infiltration of $CD8^+$ T cells in small bile ducts, and severe PBC liver lesions, whereas CD4 cells do not transfer disease.[14]

[1]Division of Rheumatology, Allergy and Clinical Immunology, University of California, Davis, California, USA; [2]Department of Pathogenic Biology and Immunology, Guangzhou University of Chinese Medicine, Guangzhou 510006, China; [3]Center for non-infectious liver diseases, Beijing 302 Hospital, Beijing 100039, China; [4]Department of Rheumatology and Immunology, The First Affiliated Hospital of Anhui Medical University, Hefei 230022, China and [5]Division of Immunology, Allergy and Rheumatology, University of Cincinnati, Cincinnati, OH 45267
[6]Co-first author.
[7]Current address: Department of Hematopathology, The University of Texas MD Anderson Cancer Center, Houston, TX, USA.
Correspondence: Dr W Zhang, PhD or ME Gershwin, MD, Division of Rheumatology, Allergy and Clinical Immunology, University of California at Davis School of Medicine, 451 Health Sciences Drive, Suite 6510, Davis, CA 95616, USA.
E-mail: ddzhang@ucdavis.edu or megershwin@ucdavis.edu
Received: 15 August 2017; Revised: 7 November 2017; Accepted: 7 November 2017

Global analysis of protein expression has lagged global gene expression analysis, but the SOMAscan proteomic assay overcomes some of the technical difficulties. SOMAscan utilizes a new generation of protein-capture SOMAmer (Slow Off-rate Modified Aptamer) reagents constructed with chemically modified nucleotides that greatly expand the physicochemical diversity of large, randomized nucleic acid libraries.[15,16] The SOMAscan Assay measures native proteins in complex matrices by transforming each individual protein concentration into a corresponding SOMAmer reagent concentration, which is then quantified by standard DNA techniques such as microarrays and qPCR.[17] Herein, we took advantage of SOMAscan technology to identify differential protein expression contributing to the development of dnTGFβRII $CD8^+$ T cell-mediated autoimmune cholangitis.

MATERIALS AND METHODS

Mice

A dnTGFβRII colony on a B6 background (B6.Cg-Tg (Cd4-TGFβR2)16Flv/J) is maintained at the University of California, Davis, animal facility (Davis, CA, USA) and bred as hemizygotes. C57BL/6J (B6) and B6.129S7-$Rag1^{tm1Mom}$/J ($Rag1^{-/-}$) mice were purchased from Jackson Laboratory (Bar Harbor, ME). dnTGFβRII mice were fed sterile rodent Helicobacter Medicated Dosing System (three-drug combination) diets (Bio-Serv, Frenchtown, NJ, USA). Sulfatrim (Hi-Tech Pharmacal, Amityville, NY, USA) was delivered through drinking water according to the manufacturer's instructions. All mice were maintained in individually ventilated cages under specific pathogen-free conditions. The experimental protocols were approved by the University of California Animal Care and Use Committee.

Adoptive cell transfer

For adoptive $CD8^+$ cell transfer, mononuclear cells were collected from the spleens of 16-week-old female dnTGFβRII mice by density gradient centrifugation using Histopaque-1.077. CD8+ cells were purified by positive selection with CD8 microbeads (Miltenyi Biotec, Auburn, CA, USA). A total of 1×10^6 purified $CD8^+$ cells was injected intravenously into eight- to ten-week-old female recipient $Rag1^{-/-}$ mice. The spleen and non-perfused liver were harvested from the recipients 8 weeks after adoptive cell transfer, and hepatic $CD8^+$ cells were purified by positive selection with CD8 microbeads, as described above.

Biological sample preparations

Whole blood was collected in EDTA-treated tubes from B6 and dnTGFβRII mice at ages of 4 and 12 weeks. The blood was centrifuged at $1500 \times g$ for 10 min at 4 °C to collect plasma; $CD8^+$ cell lysates were prepared using M-PER Mammalian Protein Extraction Reagent (ThermoFisher Scientific, Rockford, IL, USA).

SOMAscan proteomic profiling

Proteomic measurements were performed at SomaLogic Inc. (Boulder, CO), using a SOMAscan assay platform. In total, 1 129 protein analytes were measured in an assay (Supplementary Table S1) that quantifies protein abundance over 8 logs (from femtomolar to micromolar), with excellent reproducibility (4.6 median %CV).

Gene ontology (GO), pathway and protein interaction analysis

The top significantly expressed proteins ($q < 0.01$) were subjected to GO, pathway and protein interaction analysis. DAVID Bioinformatics Resources 6.7[18] (https://david.ncifcrf.gov/) was used for data input, Gene Ontology and pathway analysis. 'Count = 3' was set as a threshold. AmiGO2 (http://amigo.geneontology.org/amigo) and PANTHER (http://pantherdb.org/) were used for further Gene Ontology analysis.[19] KEGG (http://www.genome.jp/kegg/) was used for pathway analysis.[20] Gene Ontology-analyzed data were visualized by Revigo[21] (http://revigo.irb.hr/). Protein interactions were analyzed by STRING v10[22] (http://string-db.org/) with a confidence score fixed at 0.4 (medium level).

Immunoblotting

Splenic and hepatic $CD8^+$ cells were purified by positive selection with CD8 microbeads, and proteins were extracted using M-PER, as described above. Immunoblotting was performed with the SDS-PAGE electrophoresis system. Briefly, 20 µl of $CD8^+$ cell lysate was electrophoresed on 4–12% NuPAGE Nove Bis-Tris gels with NuPAGE MOPS SDS running buffer and then transferred to nitrocellulose membranes. Membranes were blocked in PBST containing 3% skim milk for 2 hours at 4 °C and then incubated with primary rabbit monoclonal antibodies against Btk, Lyn and β-Actin (Cell Signaling, Beverly, MA, USA) overnight at 4 °C. The membranes were washed in PBST, incubated with horseradish peroxidase-labeled anti-rabbit antibody (Cell Signaling, Beverly, MA, USA) and developed with SuperSignal Chemiluminescent Substrates (ThermoFisher Scientific, Rockford, lL, USA). Membranes were restored using Restore PLUS Western Blot Stripping Buffer (ThermoFisher Scientific) and reprobed. Densitometry was measured with ImageJ software. Relative Btk and Lyn band intensity was normalized and quantified. The housekeeping protein β-Actin was used as the control.

Statistical analysis

Quantitative data are presented as medians. Multiple comparison corrections were performed using the false discovery rate (FDR) methodology. A two-sided Student's *t*-test was used to determine significant changes in abundance (FDR corrected q value (q) < 0.05). One-way analysis of variance (ANOVA) was used to statistically analyze immunoblotting data. A *P* value of 0.05 or less was considered statistically significant. Fisher's exact test was used to evaluate whether the proportions of the proteins in each category differed by group.

RESULTS

The serum protein expression profile differed in dnTGFβRII mice compared to B6 mice

The serum protein expression profiles in 4- and 12-week-old dnTGFβRII mice and B6 mice ($n=8$ each time point) were analyzed using the SOMAscan platform (Supplementary Table S1). Protein abundance is shown in Figure 1a. A total of 115 proteins were differentially expressed, including 54 proteins that were significantly increased and 61 proteins that were significantly decreased in the serum of 12-week-old dnTGFβRII mice compared to that of 4-week-old dnTGFβRII mice (Figure 1b). The top 38 differentially expressed proteins ($q<0.01$) were assigned to 7 functional annotation categories (Table 1). Additionally, 87 proteins were significantly increased, and 45 proteins were significantly decreased in the serum of 12-week-old dnTGFβRII mice compared with that of 12-week-old B6 mice. Of those, the top 45 differentially expressed proteins ($q<0.01$) were assigned to 61 functional annotation categories (Supplementary Table S2). Only 3 overexpressed proteins were found in the serum of 4-week-old dnTGFβRII mice compared with that of 4-week-old B6 mice, consistent with minimal disease in dnTGFβRII mice at this early age.[23] IL18bp (Interleukin 18 Binding Protein) was increased in both 4- and 12-week-old dnTGFβRII mice. Among the differentially expressed proteins in the serum of 12-week-old dnTGFβRII mice vs. 4-week-old dnTGFβRII mice, seventy-eight proteins,

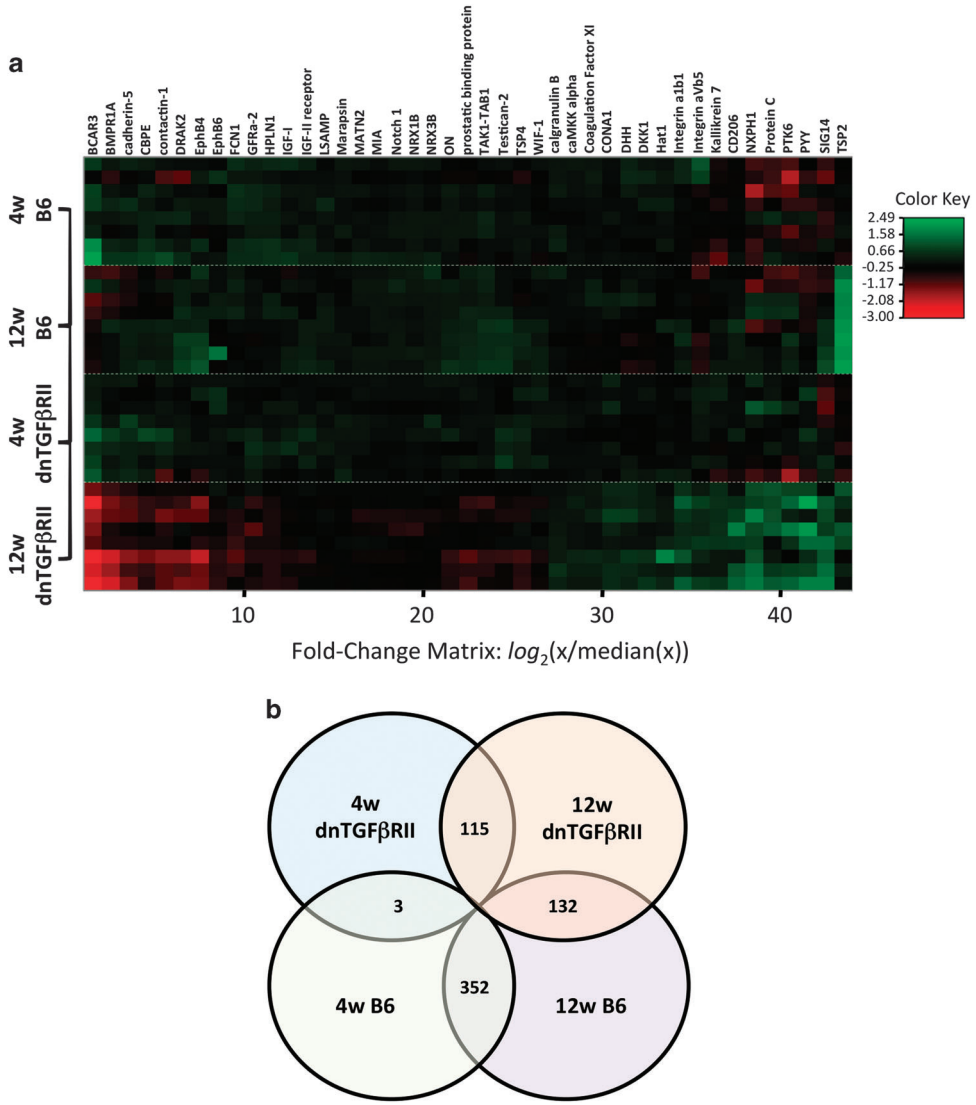

Figure 1 Differentially expressed proteins in dnTGFβRII mouse sera. (**a**) Heat map representing protein abundance in 4- and 12-week-old dnTGFβRII mouse sera and 4- and 12-week-old B6 mouse sera by the SOMAscan platform. The samples were present in rows and separated into 4- and 12-week-old dnTGFβRII (4w-dnTGFβRII, 12w-dnTGFβRII) and 4- and 12-week-old B6 (4w-control, 12w-control). The proteins that presented in columns were ordered by hierarchical clustering. Red represents more abundant proteins, and green represents less abundant proteins. (**b**) The number of altered serum proteins in 4- and 12-week-old dnTGFβRII sera compared to 4- and 12-week-old B6 sera.

including IgG, IFN-γ and IL-2 sRγ (IL-2 soluble receptor gamma), were increased in dnTGFβRII mice but not B6 mice (12-week-old vs 4-week-old B6 mice) (Supplementary Table S3). Consistent with a previous proteomic study,[24] the number of protein alterations in the serum of 4-week-old and 12-week-old B6 mice was greater than that in either 4- or 12-week-old

Table 1 The GO analysis results of serum proteins differentially expressed between 4w and 12w dnTGFβRII mice

NO	*Category*	*GO Term*	*Count*	*Gene Symbol of Proteins*
1	GO:0006468	protein amino acid phosphorylation	7	Rps6ka5, Fyn, Mapk3, Camk2d, Csk, Prkcb, Btk
2	GO:0016310	phosphorylation	7	Rps6ka5, Fyn, Mapk3, Camk2d, Csk, Prkcb, Btk
3	GO:0042127	regulation of cell proliferation	6	Hmgb1, Fgf7, Ptgs2, Fgf16, Sparc, Csk
4	GO:0006793	phosphorus metabolic process	7	Rps6ka5, Fyn, Mapk3, Camk2d, Csk, Prkcb, Btk
5	GO:0006796	phosphate metabolic process	7	Rps6ka5, Fyn, Mapk3, Camk2d, Csk, Prkcb, Btk
6	GO:0007169	transmembrane receptor protein tyrosine kinase signaling pathway	3	Fgf7, Fgf16, Angpt2
7	GO:0006508	proteolysis	6	Eml2, Klk7, Rnf123, Acy1, Bmp1, Pappa

Count: the number of proteins with altered expression within the individual GO category.

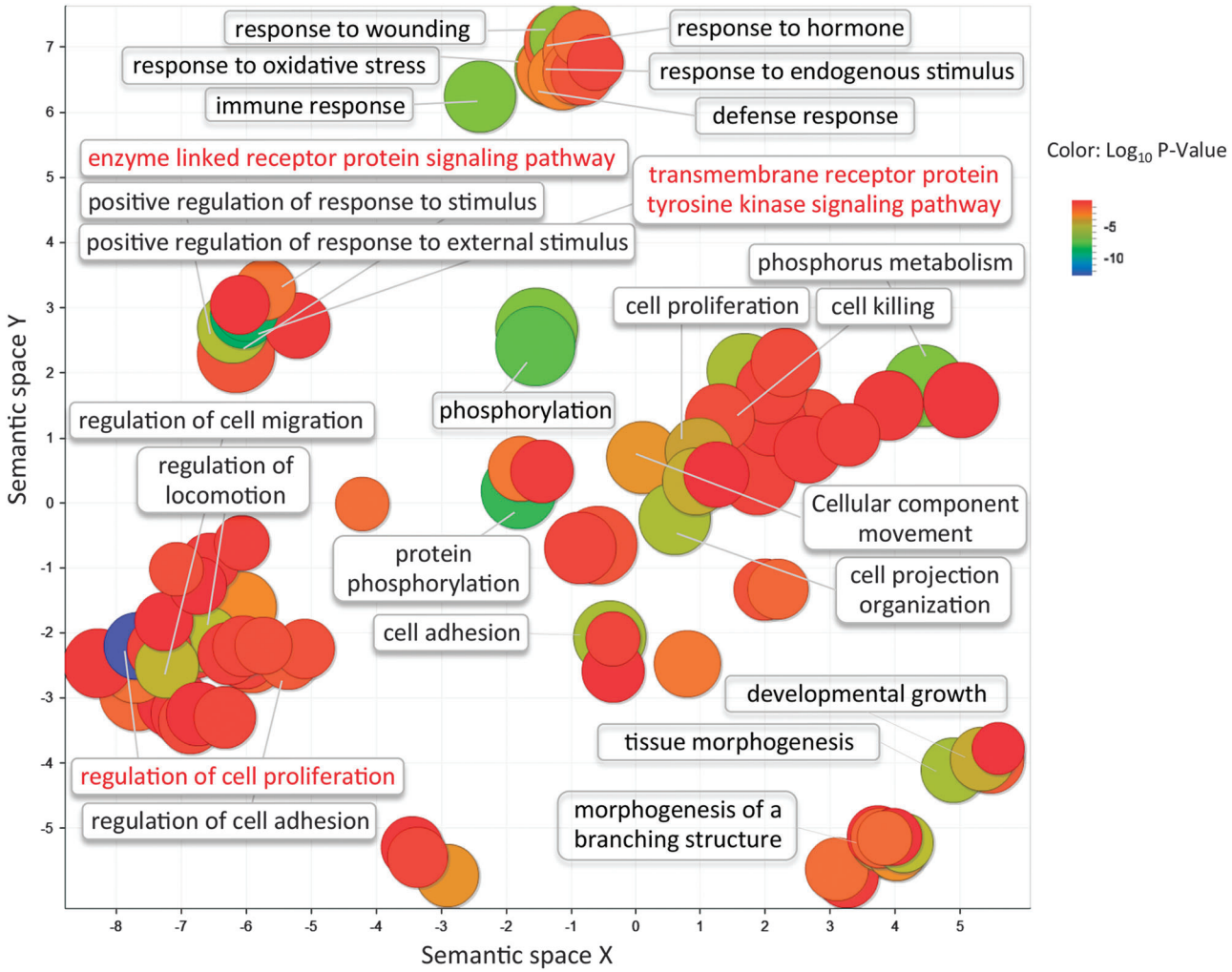

Figure 2 Semantic similarity-based scatterplots of GO terms of differentially expressed proteins between donor splenic and recipient hepatic CD8$^+$ cells. GO terms of differentially expressed proteins and the *P* value for each GO term, generated by DAVID Bioinformatics Resources 6.7, were used by Revigo to produce the scatter plots. Multi-dimensional scaling was used to reduce the dimensionality of a matrix of the GO terms' pairwise semantic similarities. The 3 most highly significant GO terms (highlighted in red) were regulation of cell proliferation (GO:0042127), $P=2.18\times10^{-13}$; enzyme linked receptor protein signaling pathway (GO:0007167), $P=1.89\times10^{-9}$; transmembrane receptor protein tyrosine kinase signaling pathway (GO:0007169), $P=2.92\times10^{-9}$.

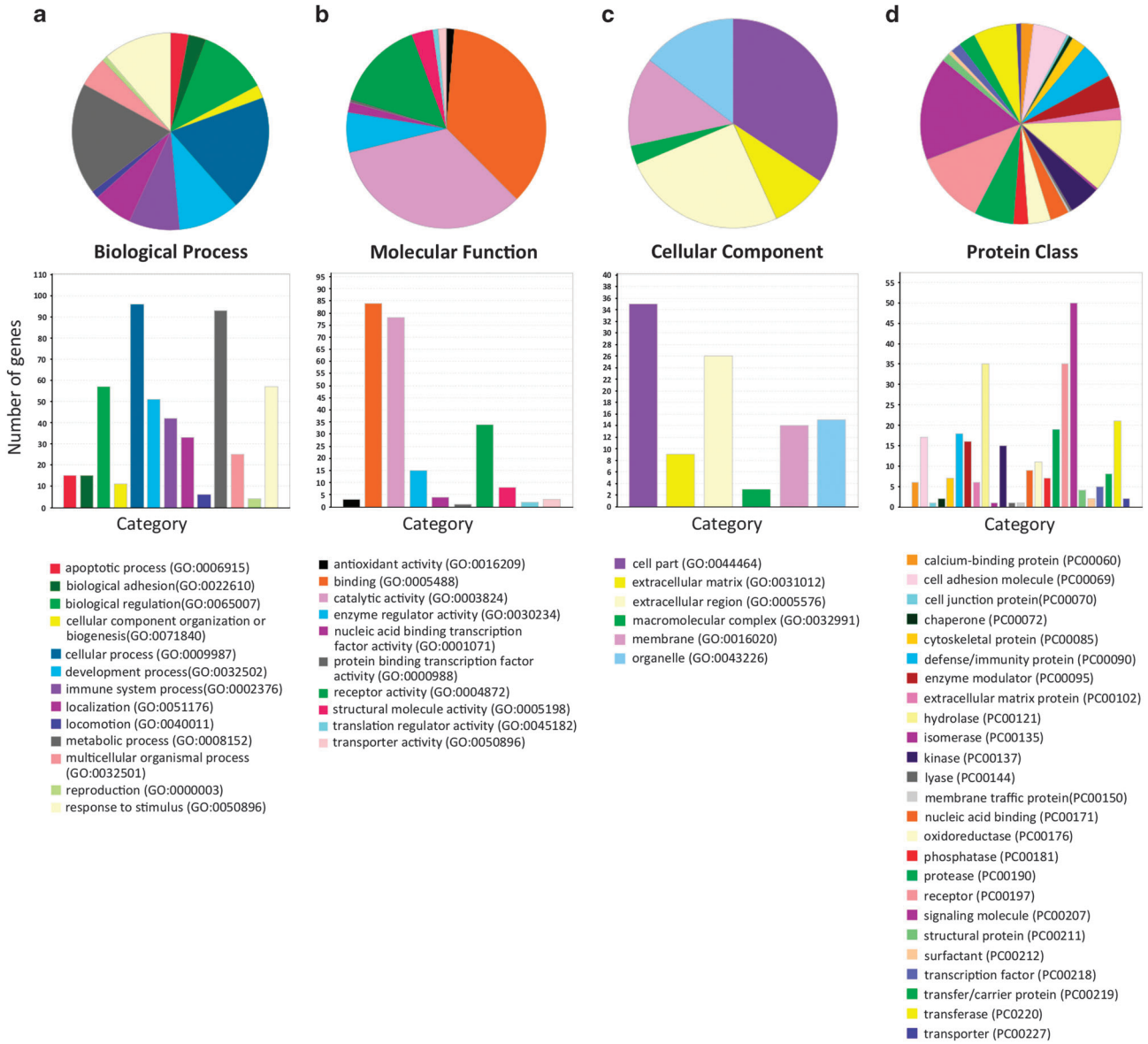

Figure 3 Functional categories of altered proteins between donor splenic and recipient liver-infiltrating CD8$^+$ cells. The gene symbols of altered proteins were used by AmiGO2 and PANTHER to produce the functional categories. (**a**): biological process, (**b**): molecular function, (**c**): molecular component, (**d**): protein class. The pie chart area represents the percentage of gene hits against total hits of the functional category.

dnTGFβRII mice, indicating the magnitude of protein changes during development in the presence and absence of autoimmunity.

Protein expression profile of dnTGFβRII CD8$^+$ cells after adoptive transfer

To further understand the critical role of CD8$^+$ cells in PBC, we next investigated the protein expression profile of dnTGFβRII mouse CD8$^+$ cells before and after adoptive transfer into Rag1$^{-/-}$ mice. We isolated CD8$^+$ cells from 16-week-old (after disease onset) dnTGFβRII mouse (donor) spleens and transferred them into Rag1$^{-/-}$ mice. The protein expression profile of CD8$^+$ cells from the paired spleens of donor mice and the livers of Rag1$^{-/-}$ mice was then analyzed eight weeks post-transfer. In total, 254 proteins were significantly increased, and 216 proteins were significantly decreased in recipient liver-resident CD8$^+$ cells compared to donor splenic CD8$^+$ cells. Gene Ontology assigned 199 differentially expressed proteins ($q<0.01$) to 359 functional annotation categories (Figure 2). Most of the differentially expressed proteins participate in responses to external or internal stimuli, the regulation of internal biological process, and the regulation of cellular morphology and activity. The differentially expressed proteins were involved in four functional categories, including biological processes, molecular functions, and molecular components (Figure 3). KEGG is a collection of manually drawn

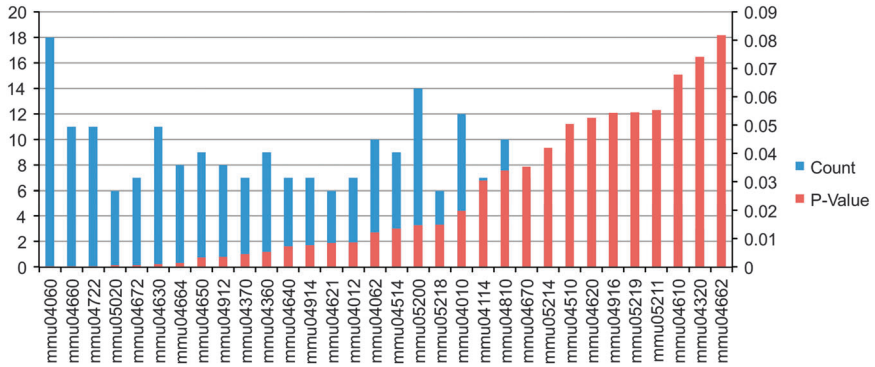

Figure 4 Results of the KEGG analysis of altered protein expression between donor splenic and recipient hepatic CD8$^+$ cells. X-axis: KEGG pathway terms. The corresponding pathway names and involved proteins are shown in Table 2. Count: the number of altered expressed proteins. *P* value: Determined by Fisher's exact test to evaluate whether the proportions of the proteins in each category differed by group.

pathway maps representing the present knowledge of molecular interaction and reaction networks. Thirty-two pathways were identified from those significantly differentially expressed proteins using KEGG analysis (Figure 4) (Table 2).

Four pathways (chemokine signaling pathway, focal adhesion pathway, T cell receptor signaling pathway and natural killer cell-mediated cytotoxicity) closely related to CD8+ cell functions were investigated in more detail (Table 3) (Supplementary Figure S1). CCL17 (decreased), CCL20 (increased), CCL27 (decreased), CCL8 (increased) and CXCL1 (decreased) were the key chemokines in this pathway identified as differentially expressed between donor splenic and recipient hepatic CD8 cells. Mapk1, Csf2, Map2k1, Fyn and Mapk11 were increased, while IL-4, Pak7, Ptpn6, Mapk12, Icos and Il2 were decreased in the T cell receptor-signaling pathway (Supplementary Figure S1). Icam1, Mapk1, Csf2, Map2k1, Fyn, and Rac1 were increased, while Ptpn6, Ncr1 and Ptpn11 were decreased in the natural killer cell-mediated cytotoxicity pathway. The altered expression of these proteins in recipient dnTGFβRII hepatic vs. donor splenic CD8 cells suggests that they might be involved in CD8 cell-mediated biliary pathological processes.

The protein expression profile of CD8+ cells differed among paired donor spleen, recipient spleen and recipient liver. We further investigated the protein expression profile in recipient splenic CD8 cells compared to donor splenic and recipient hepatic CD8 cells. In striking contrast to the large number of protein expression differences between dnTGFβRII donor splenic CD8 cells and recipient hepatic CD8 cells, there was minimal difference between recipient splenic CD8 and recipient hepatic CD8 cells; only 5 proteins showed decreased expression in recipient hepatic CD8 cells compared to splenic CD8 cells (Figures 5a and b) (Table 4), suggesting that intrinsic alterations of dnTGFβRII CD8 cells occur *in vivo*, which could predispose recipients to disease. The Lynb (an isoform of Lyn), Lyn and Btk proteins are tyrosine kinases and are critical for immune responses.[25,26] Importantly, KEGG pathway analysis suggested that Lyn and Btk were both involved in the NF-κB signaling pathway, as shown in Table 5. We therefore focused on Lyn and Btk and compared their expression levels in splenic and hepatic CD8 cells. Due to extremely low yields of hepatic CD8 cells compared to those of splenic CD8 cells, two independent cell preparations were used to compare between dnTGFβRII and B6 mice. Immunoblotting analysis of splenic and hepatic CD8 cells demonstrated markedly decreased expression of Lyn and Btk in dnTGFβRII hepatic CD8 cells compared to B6 hepatic CD8 cells (Figures 5c and d).

DISCUSSION

Several murine models of autoimmune cholangitis have attracted considerable attention because they have enabled observations at the earliest phases of disease development.[27–31] In the work described herein, we focused on dnTGFβRII mice, and the data indicate kinetic variations in the serum proteomic profile in dnTGFβRII mice and B6 mice. Comparing the differentially expressed proteins in 12-week-old B6 mice vs 12-week-old dnTGFβRII mice to the differentially expressed proteins in 4-week-old B6 mice vs 4-week-old dnTGFβRII mice, only IL18bp (interleukin 18 binding protein) was increased in both cases. Our data suggest that IL18bp may be one of the earliest proteins affected by aberrant TGF-β signaling in dnTGFβRII mice. IL18bp, a secreted protein, is overexpressed in C3H/HeJ mice with Alopecia areata.[32] IL18bp binds to IL-18 (interleukin-18) and inhibits its activity.[33]

IL-18 is a known interferon-gamma (IFN-γ)-inducing factor. Elevated expression of IL-18, which is known to have proinflammatory functions, has been implicated in autoimmune hepatitis,[34] systemic lupus erythematosus,[35] Crohn's disease, psoriasis, type-1 diabetes, rheumatoid arthritis, macrophage activation syndrome[35,36] and autoinflammatory diseases driven by the inflammasome.[37] IFN-γ augments the gene expression and synthesis of IL18bp[38] and therefore contributes to a negative feedback loop.[36] TGF-β suppresses the production of IL-18 and IFN-γ through regulation of the IL-18 receptor[39] and the degradation of IFN-γ mRNA.[40] Indeed, IFN-γ is increased in 12-week-old dnTGFβRII mouse serum when

Table 2 Thirty-two pathways identified from differentially expressed proteins between donor splenic and recipient hepatic CD8+ cells by KEGG pathway analysis

NO	*KEGG entry*	*Pathway name*	*Gene Symbol*
1	mmu04060	Cytokine-cytokine receptor interaction	Il4, Cxcl1, Csf2, Il18r1, Il22ra1, Tnfrsf13b, Tnfrsf13c, Ccl8, Kit, Il24, Tnfsf9, Ccl17, Tnfsf8, Il10rb, Il15ra, Bmp7, Cd27, Il2
2	mmu04660	T cell receptor signaling pathway	Il4, Mapk1, Pak7, Ptpn6, Csf2, Mapk12, Map2k1, Fyn, Icos, Mapk11, Il2
3	mmu04722	Neurotrophin signaling pathway	Ntrk3, Mapk1, Bdnf, Mapk12, Map2k1, Bcl2, Rac1, Camk2d, Mapk11, Camk2a, Ptpn11
4	mmu05020	Prion diseases	Mapk1, Notch1, C9, Map2k1, Fyn, Stip1
5	mmu04672	Intestinal immune network for Ig production	Il4, Icos, Tnfrsf13b, Tnfrsf13c, Il15ra, Pigr, Il2
6	mmu04630	Jak-STAT signaling pathway	Il4, Tyk2, Ptpn6, Csf2, Il22ra1, Il10rb, Il15ra, Jak2, Il24, Il2, Ptpn11
7	mmu04664	Fc epsilon RI signaling pathway	Il4, Mapk1, Csf2, Mapk12, Map2k1, Fyn, Rac1, Mapk11
8	mmu04650	Natural killer cell mediated cytotoxicity	Icam1, Mapk1, Ptpn6, Csf2, Map2k1, Fyn, Rac1, Ncr1, Ptpn11
9	mmu04912	GnRH signaling pathway	Mapk1, Mapk12, Map2k1, Gnrh1, Camk2d, Hbegf, Mapk11, Camk2a
10	mmu04370	VEGF signaling pathway	Mapk1, Mapk12, Map2k1, Ptgs2, Rac1, Mapkapk3, Mapk11
11	mmu04360	Axon guidance	Mapk1, Pak7, Efnb3, Fyn, Rac1, Cfl1, Unc5d, Ephb4, Epha3
12	mmu04640	Hematopoietic cell lineage	Il4, Csf2, Cd36, Cd33, Cd22, Kit, Itga2b
13	mmu04914	Progesterone-mediated oocyte maturation	Ccnb1, Hsp90ab1, Mapk1, Mapk12, Map2k1, Plk1, Igf1, Mapk11
14	mmu04621	NOD-like receptor signaling pathway	Hsp90ab1, Cxcl1, Mapk1, Mapk12, Ccl8, Mapk11
15	mmu04012	ErbB signaling pathway	Mapk1, Pak7, Map2k1, Erbb4, Camk2d, Hbegf, Camk2a
16	mmu04062	Chemokine signaling pathway	Cxcl1, Mapk1, Map2k1, Ccl20, Fgr, Hck, Rac1, Ccl8, Jak2, Ccl17
17	mmu04514	Cell adhesion molecules (CAMs)	Icam1, Cadm3, Nrxn3, Icos, Pecam1, Cd22, Nrxn1, Cdh2, Jam2
18	mmu05200	Pathways in cancer	Hsp90ab1, Mapk1, Fgf5, Fgf8, Fgfr3, Map2k1, Ptgs2, Bcl2, Rac1, Igf1, Kit, Fgf20, Wnt7a, Itga2b
19	mmu05218	Melanoma	Mapk1, Fgf5, Fgf8, Map2k1, Igf1, Fgf20
20	mmu04010	MAPK signaling pathway	Mapk1, Fgf5, Bdnf, Fgf8, Fgfr3, Mapk12, Map2k1, Mapkapk5, Rac1, Mapkapk3, Mapk11, Fgf20
21	mmu04114	Oocyte meiosis	Ccnb1, Mapk1, Mapk12, Map2k1, Plk1, Camk2d, Igf1, Camk2a
22	mmu04810	Regulation of actin cytoskeleton	Mapk1, Pak7, Fgf5, Fgf8, Fgfr3, Map2k1, Rac1, Cfl1, Fgf20, Itga2b
23	mmu04670	Leukocyte transendothelial migration	Icam1, Mapk12, Pecam1, Rac1, Mapk11, Jam2, Ptpn11
24	mmu05214	Glioma	Mapk1, Map2k1, Camk2d, Igf1, Camk2a
25	mmu04510	Focal adhesion	Mapk1, Pak7, Map2k1, Fyn, Bcl2, Rac1, Igf1, Thbs1, Itga2b
26	mmu04620	Toll-like receptor signaling pathway	Mapk1, Mapk12, Map2k1, Rac1, Mapk11, Lbp
27	mmu04916	Melanogenesis	Mapk1, Map2K1, Camk2D, Kit, Camk2a, Wnt7a
28	mmu05219	Bladder cancer	Mapk1, Fgfr3, Map2k1, Thbs1
29	mmu05211	Renal cell carcinoma	Mapk1, Pak7, Map2k1, Rac1, Ptpn11
30	mmu04610	Complement and coagulation cascades	C9, C4a, F9, Cpb2, Plg
31	mmu04320	Dorso-ventral axis formation	Mapk1, Notch1, Map2k1
32	mmu04662	B cell receptor signaling pathway	Mapk1, Ptpn6, Map2k1, Rac1, Cd22

compared with 4-week-old dnTGFβRII mice. Therefore, the increase in IL18bp may be due to a chronic elevation in IFN-γ in dnTGFβRII mice.

Bmp1 (bone morphogenetic protein 1) and Nrxn3 (neurexin III) were decreased in both 4- and 12-week-old dnTGFβRII serum compared to 4- and 12-week-old B6 serum. Bmp1 is a metalloproteinase that cleaves multiple extracellular matrix proteins and activates TGF-β by releasing it from a secreted large latent complex (LLC).[41] Since TGF-β induces Bmp1 mRNA and protein expression,[42] these two proteins are involved in a positive amplification loop.[41] Thus, the decrease in Bmp1 is due to lack of TGF-β signaling and could be a biomarker of PBC-like disease induced by blockage of TGF-β signaling. Nrxn3 is a protein involved in cell adhesion and the nervous system. Forkhead box Q1 (Foxq1) directly binds to the Nrxn3 promoter and suppresses Nrxn3 expression,[43] while TGF-β induces the production of Foxq1.[44] The decreased expression of Nrxn3 in 12-week-old dnTGFβRII mice indicated

Table 3 The pathways related to CD8$^+$ cells and corresponding proteins that are altered in recipient hepatic CD8$^+$ cells in comparison to donor splenic CD8$^+$ cells

KEGG entry	*Pathway name*	*Protein*	*Gene Symbol*	*Log_2FC*
mmu 04062	Chemokine signaling pathway	Janus kinase 2	Jak2	0.034
		FGR proto-oncogene, Src family tyrosine kinase	Fgr	0.138
		mitogen-activated protein kinase 1	Map2k1	0.085
		mitogen-activated protein kinase 1	Mapk1	0.021
		RAS-related C3 botulinum substrate 1	Rac1	0.053
		chemokine (C-C motif) ligand 17	Ccl17	−0.051
		chemokine (C-C motif) ligand 20	Ccl20	0.054
		chemokine (C-C motif) ligand 27	Ccl27	−0.026
		chemokine (C-C motif) ligand 8	Ccl8	0.077
		chemokine (C-X-C motif) ligand 1	Cxcl1	−0.047
mmu 04510	Focal adhesion pathway	mitogen-activated protein kinase 1	Mapk1	0.021
		p21 protein (Cdc42/Rac)-activated kinase 7	Pak7	−0.036
		mitogen-activated protein kinase 1	Map2k1	0.085
		Fyn proto-oncogene	Fyn	0.123
		B cell leukemia/lymphoma 2	Bcl2	−0.056
		RAS-related C3 botulinum substrate 1	Rac1	0.053
		insulin-like growth factor 1	Igf1	0.164
		thrombospondin 1	Thbs1	−0.028
		integrin alpha 2b	Itga2b	−0.099
mmu 04660	T cell receptor signaling pathway	interleukin 4	Il4	−0.021
		mitogen-activated protein kinase 1	Mapk1	0.021
		p21 protein (Cdc42/Rac)-activated kinase 7	Pak7	−0.036
		protein tyrosine phosphatase, non-receptor type 6	Ptpn6	−0.093
		colony stimulating factor 2 (granulocyte-macrophage)	Csf2	0.084
		mitogen-activated protein kinase 12	Mapk12	−0.036
		mitogen-activated protein kinase 1	Map2k1	0.085
		Fyn proto-oncogene	Fyn	0.123
		inducible T cell co-stimulator	Icos	−0.020
		mitogen-activated protein kinase 11	Mapk11	0.051
		interleukin 2	Il2	−0.044
mmu 04650	Natural killer cell mediated cytotoxicity	intercellular adhesion molecule 1	Icam1	0.037
		mitogen-activated protein kinase 1	Mapk1	0.021
		protein tyrosine phosphatase, non-receptor type 6	Ptpn6	−0.093
		colony stimulating factor 2 (granulocyte-macrophage)	Csf2	0.084
		mitogen-activated protein kinase 1	Map2k1	0.085
		Fyn proto-oncogene	Fyn	0.123
		RAS-related C3 botulinum substrate 1	Rac1	0.053
		natural cytotoxicity triggering receptor 1	Ncr1	−0.042
		protein tyrosine phosphatase, non-receptor type 11	Ptpn11	−0.087

FC stands for fold change.

that defective TGF-β receptor signaling enhances, instead of inhibits, expression of Foxq1. Of note, we focused on the proteomic changes that may contribute to the initiation of disease in 12-week-old dnTGFβRII mice, which display mild portal inflammation and no obvious histological features of liver injury in contrast to 24-week-old mice with established disease. However, the levels of proinflammatory cytokines such as TNF-α, IL-6 and IL-12 increased but did not reach statistical significance (data not shown) in sera from 12-week-old dnTGFβRII mice when compared to either 4-week-old dnTGFβRII mice or 12-week-old B6 mice.

We also identified CD8 cell proteins that showed altered expression between recipient liver and donor spleens. Gene Ontology analysis (Figure 3) showed that some of these proteins participate in responses to external or internal stimuli, the regulation of internal biological processes, and cellular morphology, activity and growth. The gene expression profiles and cellular differentiation of CD8$^+$ cells are determined by antigen strength, co-stimulatory molecules and cytokines.[45]

Analysis of the 'natural killer cell-mediated cytotoxicity pathway' indicates that the cytotoxicity mediated by NK cells is enhanced. Cells isolated from mouse spleen or liver using

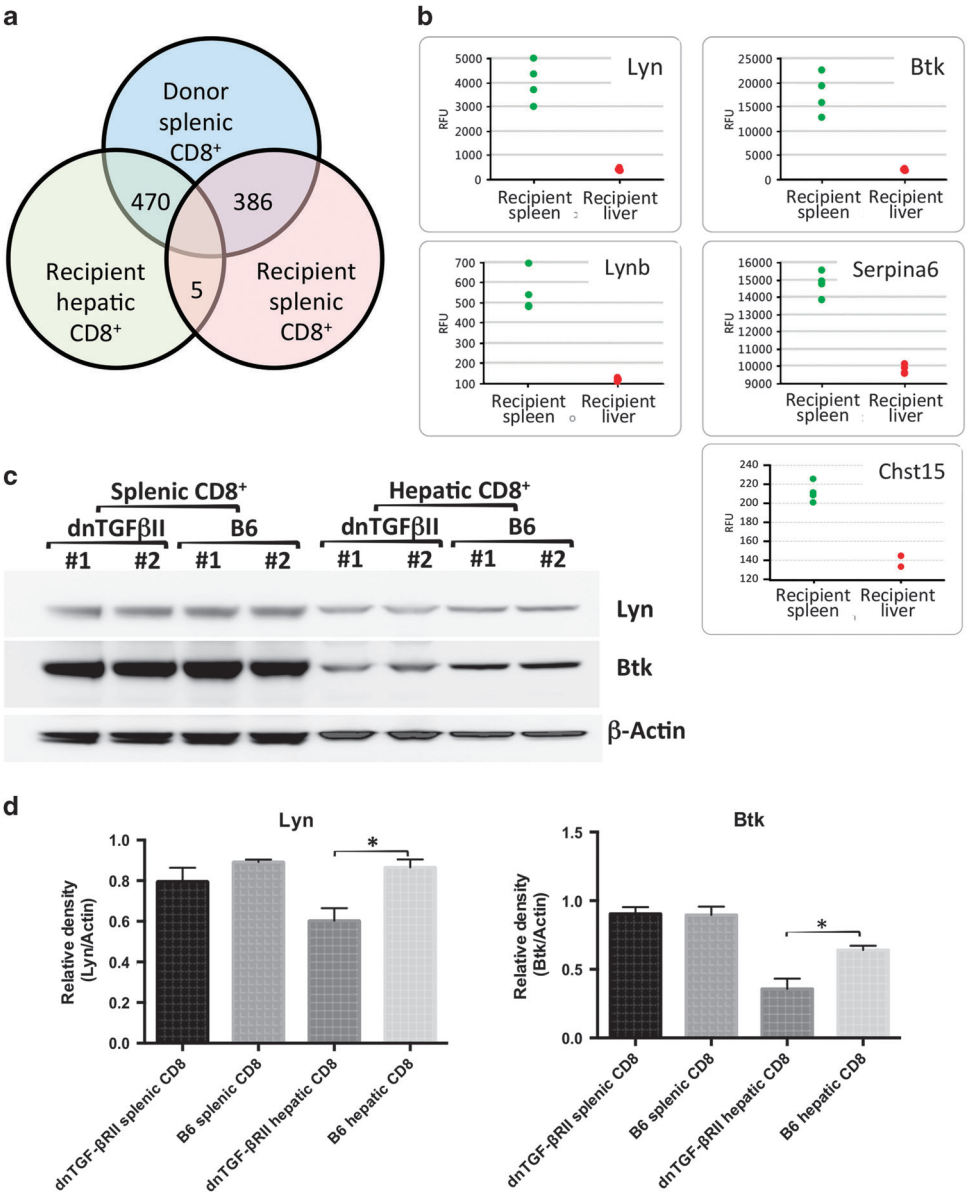

Figure 5 Comparison of differentially expressed proteins in splenic and hepatic CD8 cells. (**a**) The number of altered proteins in CD8$^+$ cells from dnTGFβRII donor spleen, recipient spleen and recipient liver ($P<0.001$, $q<0.05$); (**b**) Proteins significantly differentially expressed in CD8$^+$ cells from donor spleen compared to recipient spleen. The protein profiles of CD8$^+$ cells from donor spleen compared to recipient spleen were analyzed by SOMAscan assay. A two-sided Student's *t*-test was used to determine the difference between two groups. All the significantly differentially expressed proteins with $q<0.01$ are shown. Relative fluorescence units (RFUs) are directly proportional to the amount of target protein in the initial sample, as informed by a standard curve generated for each protein-SOMAmer pair. (**c**) Immunoblotting analysis of Btk and Lyn expression levels in splenic and hepatic CD8 cells. #1 and #2 indicate two sample preparations of CD8 cell lysates. Each preparation included a pool of CD8 cells from 3–4 dnTGFβRII mice and 8–10 B6 mice. (**d**) Densitometry analysis demonstrated the band density ratio of Btk (left panel) and Lyn (right panel) to β-Actin, respectively.

CD8 beads may contain CD8$^+$ cytotoxic T cells, CD8$^+$ regulatory T cells, naïve CD8$^+$ T cells, CD8$^+$ dendritic cells and CD8$^+$ NKT cells. Pathway analysis indicates that cytotoxic CD8$^+$ cells play an important role in inducing PBC, consistent with our previous observation that KLRG1$^+$ CD8 cells mediate cholangiocyte lysis.[10,11] NKT cells, a specialized group of T cells that recognize self, foreign lipids and glycolipids such as α-GalCer presented by the non-polymorphic MHC I-like molecule CD1d, play a critical role in immunity, tolerance and autoimmunity in the liver.[46] NKT cells accumulate in the liver of PBC patients.[47,48] NKT cells also promote PBC in mice,[49] including dnTGFβRII mice.[50] NKT cells consist of two classes: type 1 or invariant NKT (iNKT) cells express Jα24-Jα18 in humans and Vα14-Jα18 in mice, whereas type 2 cells express a variety of TCRs recognizing CD1d.[46] Both type 1 and type 2 NKT cells express NK cell stimulatory receptors, such as NK1.1 in mice and NKG2C and NKG2D in humans.[46] However, iNKT cells always down-regulate CD8 at an early stage,[51] and

Table 4 Pathway analysis of proteins differentially expressed between donor splenic and recipient splenic CD8$^+$ cells

Protein	*Gene Symbol*	*KEGG Pathway*
Fyn proto-oncogene	Fyn	mmu04510: Focal adhesion
		mmu04520: Adherens junction
		mmu04650: Natural killer cell mediated cytotoxicity
		mmu04660: T cell receptor signaling pathway
cofilin 1, non-muscle	Cfl1	mmu04810: Regulation of actin cytoskeleton
colony stimulating factor 2 (granulocyte-macrophage)	Csf2	mmu04060: Cytokine-cytokine receptor interaction
		mmu04630: Jak-STAT signaling pathway
		mmu04650: Natural killer cell mediated cytotoxicity
		mmu04660: T cell receptor signaling pathway
leukotriene A4 hydrolase	Lta4h	mmu00590: Arachidonic acid metabolism
polo-like kinase 1	Plk1	mmu04110: Cell cycle
glutamate oxaloacetate transaminase 1, soluble	Got1	mmu00250: Alanine, aspartate and glutamate metabolism
		mmu00270: Cysteine and methionine metabolism
		mmu00330: Arginine and proline metabolism
		mmu00350: Tyrosine metabolism
		mmu00360: Phenylalanine metabolism
		mmu00400: Phenylalanine, tyrosine and tryptophan biosynthesis
thioredoxin domain containing 12	Txndc12	mmu00480: Glutathione metabolism
transketolase	Tkt	mmu00030: Pentose phosphate pathway

Pathways were presented after manually filtering as described. Differentially expressed proteins with a q value less than 0.01 are listed.

Table 5 Pathway analysis of proteins differentially expressed between recipient splenic and recipient liver CD8$^+$ cells

Protein	*Gene Symbol*	*KEGG Pathway*
Yamaguchi sarcoma viral (v-yes-1) oncogene homolog	Lyns	mmu04062:Chemokine signaling pathway
		mmu04064:NF-kappa B signaling pathway
Bruton agammaglobulinemia tyrosine kinase	Btk	mmu04064:NF-kappa B signaling pathway
		mmu05340:Primary immunodeficiency

Pathways are presented after manually filtering as described.

CD8$^+$ iNKT cells are seldom detected in mice.[52] Therefore, the NKT cells in our study are unlikely to be iNKT (type I NKT) cells. It is reported that most human hepatic NKT cells are type 2 NKT cells, including CD8$^+$ NKT cells.[53] CD8$^+$ NKT cells are present in all mouse tissues except thymus,[54] and activated CD8$^+$ T cells acquire NK1.1 expression and preferentially reside in the liver of mice.[55] CD8$^+$ NKT cells, not CD8$^+$ NK1.1$^-$ cells, are able to proliferate independently from antigen stimulation and express IFN-γ and GzmB.[56] Based on these studies, the 'natural killer cell-mediated cytotoxicity' pathway may be involved in CD8-mediated biliary destruction. Type 2 CD8$^+$ NKT cells may prime PBC-like disease in mice and even in PBC patients. However, these hypotheses require more experiments *in vitro* and *in vivo* to verify.

Five proteins were decreased in recipient splenic CD8$^+$ cells compared to recipient hepatic CD8$^+$ cells (Figure 5). These proteins in CD8$^+$ cells may reflect a response to a different microenvironment (liver and spleen) or the promotion of PBC in mice. Lyn is a tyrosine protein kinase that plays a critical role in the regulation of innate and adaptive immune responses. Lyn is activated by a variety of stimuli, including BCR, CD40, LPS, cytokines, and integrins.[25] Mice without Lyn (Lyn$^{-/-}$) have circulating autoreactive antibodies,[57] which are dependent on T cells.[58] Gain-of-function Lyn mutation (Lyn (up/up) mice, which express a constitutively active form of Lyn, are more sensitive to endotoxin in a dendritic cell- and NK cell-dependent manner.[25] Btk not only plays an important role in B cell development and differentiation but also promotes TLR3-triggered NK cell (CD3$^-$NK1.1$^+$) activation, mainly by activating the NF-κB pathway, and contributes to TLR3-triggered acute liver injury.[26] Consistent with human GWASs implicating NF-κB pathway involvement in the pathogenesis of human PBC,[59] this study highlights the importance of NF-κB signaling mediated by Btk and Lyn in autoimmune cholangitis. However, the functional roles of these proteins in CD8$^+$ cells in the pathogenesis of human PBC need to be further investigated. Taken together, our data reveal that a critical serological response and distinct profiles of CD8 cells may be responsible for the development of autoimmune cholangitis.

CONFLICT OF INTEREST

The authors declare no conflict of interest.

ACKNOWLEDGEMENTS

Financial Support: Funded by National Institutes of Health grant DK090019.

1 Kaplan MM, Gershwin ME. Primary biliary cirrhosis. *N Engl J Med* 2005; **353**: 1261–1273.
2 Hirschfield GM, Gershwin ME. The immunobiology and pathophysiology of primary biliary cirrhosis. *Annu Rev Pathol* 2013; **8**: 303–330.
3 Tomiyama T, Yang GX, Zhao M, Zhang W, Tanaka H, Wang J *et al.* The modulation of co-stimulatory molecules by circulating exosomes in primary biliary cirrhosis. *Cell Mol Immunol* 2017; **14**: 276–284.
4 Kita H, Lian ZX, Van de Water J, He XS, Matsumura S, Kaplan M *et al.* Identification of HLA-A2-restricted CD8(+) cytotoxic T cell responses in primary biliary cirrhosis: T cell activation is augmented by immune complexes cross-presented by dendritic cells. *J Exp Med* 2002; **195**: 113–123.
5 Van de Water J, Ansari A, Prindiville T, Coppel RL, Ricalton N, Kotzin BL *et al.* Heterogeneity of autoreactive T cell clones specific for the E2 component of the pyruvate dehydrogenase complex in primary biliary cirrhosis. *J Exp Med* 1995; **181**: 723–733.
6 Kita H, Matsumura S, He XS, Ansari AA, Lian ZX, Van de Water J *et al.* Quantitative and functional analysis of PDC-E2-specific autoreactive cytotoxic T lymphocytes in primary biliary cirrhosis. *J Clin Invest* 2002; **109**: 1231–1240.
7 Tsuda M, Ambrosini YM, Zhang W, Yang GX, Ando Y, Rong G *et al.* Fine phenotypic and functional characterization of effector cluster of differentiation 8 positive T cells in human patients with primary biliary cirrhosis. *Hepatology* 2011; **54**: 1293–1302.
8 Fan LY, Tu XQ, Cheng QB, Zhu Y, Feltens R, Pfeiffer T *et al.* Cytotoxic T lymphocyte associated antigen-4 gene polymorphisms confer susceptibility to primary biliary cirrhosis and autoimmune hepatitis in Chinese population. *World J Gastroenterol* 2004; **10**: 3056–3059.
9 Dhirapong A, Yang GX, Nadler S, Zhang W, Tsuneyama K, Leung P *et al.* Therapeutic effect of cytotoxic T lymphocyte antigen 4/immunoglobulin on a murine model of primary biliary cirrhosis. *Hepatology* 2013; **57**: 708–715.
10 Hsu W, Zhang W, Tsuneyama K, Moritoki Y, Ridgway WM, Ansari AA *et al.* Differential mechanisms in the pathogenesis of autoimmune cholangitis versus inflammatory bowel disease in interleukin-2Ralpha (−/−) mice. *Hepatology* 2009; **49**: 133–140.
11 Huang W, Kachapati K, Adams D, Wu Y, Leung PS, Yang GX *et al.* Murine autoimmune cholangitis requires two hits: cytotoxic KLRG1(+) CD8 effector cells and defective T regulatory cells. *J Autoimmun* 2014; **50**: 123–134.
12 Gorelik L, Flavell RA. Abrogation of TGFbeta signaling in T cells leads to spontaneous T cell differentiation and autoimmune disease. *Immunity* 2000; **12**: 171–181.
13 Oertelt S, Lian ZX, Cheng CM, Chuang YH, Padgett KA, He XS *et al.* Anti-Mitochondrial Antibodies and Primary Biliary Cirrhosis in TGF-Receptor II Dominant-Negative Mice. *The Journal of Immunology* 2006; **177**: 1655–1660.
14 Yang GX, Lian ZX, Chuang YH, Moritoki Y, Lan RY, Wakabayashi K *et al.* Adoptive transfer of CD8(+) T cells from transforming growth factor beta receptor type II (dominant negative form) induces autoimmune cholangitis in mice. *Hepatology* 2008; **47**: 1974–1982.
15 Webber J, Stone TC, Katilius E, Smith BC, Gordon B, Mason MD *et al.* Proteomics analysis of cancer exosomes using a novel modified aptamer-based array (SOMAscan) platform. *Mol Cell Proteomics* 2014; **13**: 1050–1064.
16 Desai B, Dixon K, Farrant E, Feng Q, Gibson KR, van Hoorn WP *et al.* Rapid discovery of a novel series of Abl kinase inhibitors by application of an integrated microfluidic synthesis and screening platform. *J Med Chem* 2013; **56**: 3033–3047.
17 Davies DR, Gelinas AD, Zhang C, Rohloff JC, Carter JD, O'Connell D *et al.* Unique motifs and hydrophobic interactions shape the binding of modified DNA ligands to protein targets. *Proc Natl Acad Sci USA* 2012; **109**: 19971–19976.
18 Huang da W, Sherman BT, Lempicki RA. Systematic and integrative analysis of large gene lists using DAVID bioinformatics resources. *Nat Protoc* 2009; **4**: 44–57.
19 Gene Ontology C. Gene Ontology Consortium: going forward. *Nucleic Acids Res* 2015; **43**: D1049–D1056.
20 Kanehisa M, Sato Y, Kawashima M, Furumichi M, Tanabe M. KEGG as a reference resource for gene and protein annotation. *Nucleic Acids Res* 2015; **44**: D457–D462.
21 Supek F, Bosnjak M, Skunca N, Smuc T. REVIGO summarizes and visualizes long lists of gene ontology terms. *PLoS One* 2011; **6**: e21800.
22 Szklarczyk D, Franceschini A, Wyder S, Forslund K, Heller D, Huerta-Cepas J *et al.* STRING v10: protein-protein interaction networks, integrated over the tree of life. *Nucleic Acids Res* 2015; **43**: D447–D452.
23 Oertelt S, Lian ZX, Cheng CM, Chuang YH, Padgett KA, He XS *et al.* Anti-mitochondrial antibodies and primary biliary cirrhosis in TGF-beta receptor II dominant-negative mice. *J Immunol* 2006; **177**: 1655–1660.
24 Zabel C, Mao L, Woodman B, Rohe M, Wacker MA, Klare Y *et al.* A large number of protein expression changes occur early in life and precede phenotype onset in a mouse model for huntington disease. *Mol Cell Proteomics* 2009; **8**: 720–734.
25 Krebs DL, Chehal MK, Sio A, Huntington ND, Da ML, Ziltener P *et al.* Lyn-dependent signaling regulates the innate immune response by controlling dendritic cell activation of NK cells. *J Immunol* 2012; **188**: 5094–5105.
26 Bao Y, Zheng J, Han C, Jin J, Han H, Liu Y *et al.* Tyrosine kinase Btk is required for NK cell activation. *J Biol Chem* 2012; **287**: 23769–23778.
27 Bae HR, Leung PS, Tsuneyama K, Valencia JC, Hodge DL, Kim S *et al.* Chronic expression of interferon-gamma leads to murine autoimmune cholangitis with a female predominance. *Hepatology* 2016; **64**: 1189–1201.
28 Hsueh YH, Chang YN, Loh CE, Gershwin ME, Chuang YH. AAV-IL-22 modifies liver chemokine activity and ameliorates portal inflammation in murine autoimmune cholangitis. *J Autoimmun* 2016; **66**: 89–97.
29 Chang CH, Chen YC, Zhang W, Leung PS, Gershwin ME, Chuang YH. Innate immunity drives the initiation of a murine model of primary biliary cirrhosis. *PLoS One* 2015; **10**: e0121320.
30 Pollheimer MJ, Fickert P. Animal models in primary biliary cirrhosis and primary sclerosing cholangitis. *Clin Rev Allergy Immunol* 2015; **48**: 207–217.
31 Tanaka H, Yang GX, Tomiyama T, Tsuneyama K, Zhang W, Leung PS *et al.* Immunological potential of cytotoxic T lymphocyte antigen 4 immunoglobulin in murine autoimmune cholangitis. *Clin Exp Immunol* 2015; **180**: 371–382.
32 Wang E, Chong K, Yu M, Akhoundsadegh N, Granville DJ, Shapiro J *et al.* Development of autoimmune hair loss disease alopecia areata is associated with cardiac dysfunction in C3H/HeJ mice. *PLoS One* 2013; **8**: e62935.
33 Novick D, Kim SH, Fantuzzi G, Reznikov LL, Dinarello CA, Rubinstein M. Interleukin-18 binding protein: a novel modulator of the Th1 cytokine response. *Immunity* 1999; **10**: 127–136.
34 Ikeda A, Aoki N, Kido M, Iwamoto S, Nishiura H, Maruoka R *et al.* Progression of autoimmune hepatitis is mediated by IL-18-producing dendritic cells and hepatic CXCL9 expression in mice. *Hepatology* 2014; **60**: 224–236.
35 Esfandiari E, McInnes IB, Lindop G, Huang FP, Field M, Komai-Koma M *et al.* A proinflammatory role of IL-18 in the development of spontaneous autoimmune disease. *J Immunol* 2001; **167**: 5338–5347.
36 Novick D, Kim S, Kaplanski G, Dinarello CA. Interleukin-18, more than a Th1 cytokine. *Semin Immunol* 2013; **25**: 439–448.
37 van Kempen TS, Wenink MH, Leijten EF, Radstake TR, Boes M. Perception of self: distinguishing autoimmunity from autoinflammation. *Nat Rev Rheumatol* 2015; **11**: 483–492.
38 Hurgin V, Novick D, Rubinstein M. The promoter of IL-18 binding protein: activation by an IFN-gamma -induced complex of IFN regulatory factor 1 and CCAAT/enhancer binding protein beta. *Proc Natl Acad Sci U S A* 2002; **99**: 16957–16962.
39 Koutoulaki A, Langley M, Sloan AJ, Aeschlimann D, Wei XQ. TNFalpha and TGF-beta1 influence IL-18-induced IFNgamma production through regulation of IL-18 receptor and T-bet expression. *Cytokine* 2010; **49**: 177–184.
40 Inoue Y, Abe K, Onozaki K, Hayashi H. TGF-beta decreases the stability of IL-18-induced IFN-gamma mRNA through the expression of

TGF-beta-induced tristetraprolin in KG-1 cells. *Biol Pharm Bull* 2015; **38**: 536–544.
41 Ge G, Greenspan DS. BMP1 controls TGFbeta1 activation via cleavage of latent TGFbeta-binding protein. *J Cell Biol* 2006; **175**: 111–120.
42 Lee S, Solow-Cordero DE, Kessler E, Takahara K, Greenspan DS. Transforming growth factor-beta regulation of bone morphogenetic protein-1/procollagen C-proteinase and related proteins in fibrogenic cells and keratinocytes. *J Biol Chem* 1997; **272**: 19059–19066.
43 Sun HT, Cheng SX, Tu Y, Li XH, Zhang S. FoxQ1 promotes glioma cells proliferation and migration by regulating NRXN3 expression. *PLoS One* 2013; **8**: e55693.
44 Peng X, Luo Z, Kang Q, Deng D, Wang Q, Peng H *et al.* FOXQ1 mediates the crosstalk between TGF-beta and Wnt signaling pathways in the progression of colorectal cancer. *Cancer Biol Ther* 2015; **16**: 1099–1109.
45 Mittrucker HW, Visekruna A, Huber M. Heterogeneity in the differentiation and function of CD8(+) T cells. *Arch Immunol Ther Exp (Warsz)* 2014; **62**: 449–458.
46 Doherty DG. Immunity, tolerance and autoimmunity in the liver: A comprehensive review. *J Autoimmun* 2015; **66**: 60–75.
47 Chuang YH, Lian ZX, Tsuneyama K, Chiang BL, Ansari AA, Coppel RL *et al.* Increased killing activity and decreased cytokine production in NK cells in patients with primary biliary cirrhosis. *J Autoimmun* 2006; **26**: 232–240.
48 Shuai Z, Leung MW, He X, Zhang W, Yang G, Leung PS *et al*. Adaptive immunity in the liver. *Cell Mol Immunol* 2016; **13**: 354–368.
49 Mattner J, Savage PB, Leung P, Oertelt SS, Wang V, Trivedi O *et al.* Liver autoimmunity triggered by microbial activation of natural killer T cells. *Cell Host Microbe* 2008; **3**: 304–315.
50 Chuang YH, Lian ZX, Yang GX, Shu SA, Moritoki Y, Ridgway WM *et al.* Natural killer T cells exacerbate liver injury in a transforming growth factor beta receptor II dominant-negative mouse model of primary biliary cirrhosis. *Hepatology* 2008; **47**: 571–580.
51 Kim EY, Lynch L, Brennan PJ, Cohen NR, Brenner MB. The transcriptional programs of iNKT cells. *Semin Immunol* 2015; **27**: 26–32.
52 Wen X, Kim S, Xiong R, Li M, Lawrenczyk A, Huang X *et al.* A Subset of CD8alphabeta+ Invariant NKT Cells in a Humanized Mouse Model. *J Immunol* 2015; **195**: 1459–1469.
53 Kenna T, Golden-Mason L, Porcelli SA, Koezuka Y, Hegarty JE, O'Farrelly C *et al.* NKT cells from normal and tumor-bearing human livers are phenotypically and functionally distinct from murine NKT cells. *J Immunol* 2003; **171**: 1775–1779.
54 Hammond KJ, Pelikan SB, Crowe NY, Randle-Barrett E, Nakayama T, Taniguchi M *et al.* NKT cells are phenotypically and functionally diverse. *Eur J Immunol* 1999; **29**: 3768–3781.
55 Wang Y, Wang H, Xia J, Liang T, Wang G, Li X *et al.* Activated CD8 T cells acquire NK1.1 expression and preferentially locate in the liver in mice after allogeneic hematopoietic cell transplantation. *Immunol Lett* 2013; **150**: 75–78.
56 Seregin SS, Chen GY, Laouar Y. Dissecting CD8+ NKT Cell Responses to Listeria Infection Reveals a Component of Innate Resistance. *J Immunol* 2015; **195**: 1112–1120.
57 Hibbs ML, Tarlinton DM, Armes J, Grail D, Hodgson G, Maglitto R *et al.* Multiple defects in the immune system of Lyn-deficient mice, culminating in autoimmune disease. *Cell* 1995; **83**: 301–311.
58 Hua Z, Gross AJ, Lamagna C, Ramos-Hernandez N, Scapini P, Ji M *et al.* Requirement for MyD88 signaling in B cells and dendritic cells for germinal center anti-nuclear antibody production in Lyn-deficient mice. *J Immunol* 2014; **192**: 875–885.
59 Mells GF, Floyd JA, Morley KI, Cordell HJ, Franklin CS, Shin SY *et al.* Genome-wide association study identifies 12 new susceptibility loci for primary biliary cirrhosis. *Nat Genet* 2011; **43**: 329–332.

Supplementary Information for this article can be found on the *Cellular & Molecular Immunology* website (http://www.nature.com/cmi)